HNPS Advances in Nuclear Physics

Vol 10 (1999)

HNPS1999

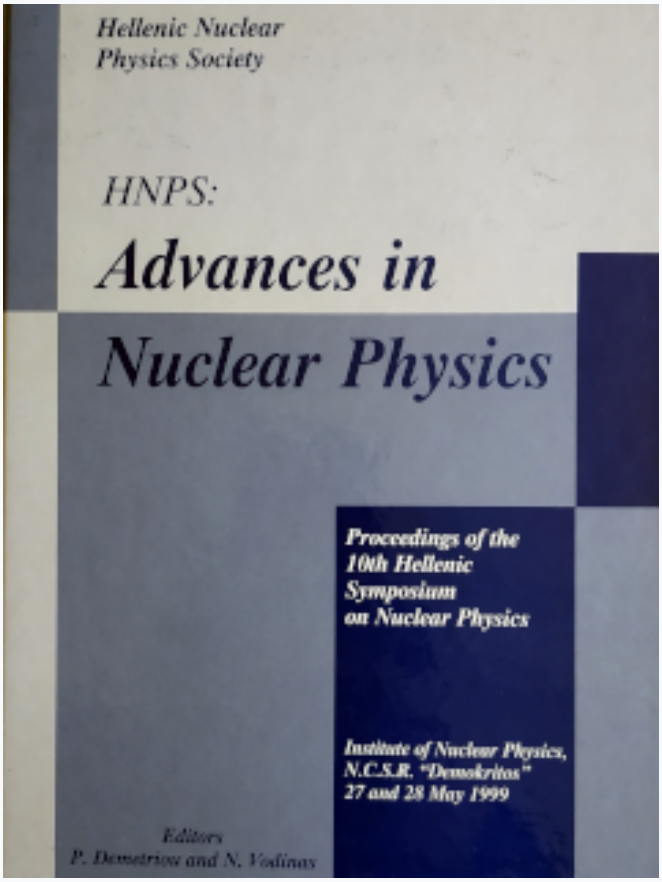

Effective Interactions: Resonances and Off-Shell Characteristics

S. E. Massen, S. A. Sofianos, S. A. Rakityansky, S. Oryu

doi: 10.12681/hnps.2177

Effective Interactions: Resonances and Off-Shell Characteristics

S.E. Massen[a,1], S.A. Sofianos[a], S.A. Rakityansky[a] and S. Oryu[b]

[a] *Physics Department, University of South Africa, P.O.Box 392, Pretoria 0003, South Africa*

[b] *Department of Physics, Science University of Tokyo, 2641 Yamazaki, Noda, Chiba 278-8510, Japan*

Abstract

The influence of resonances on the analytical properties and off-shell characteristics of effective interactions has been investigated. This requires, among others, the knowledge of the Jost function in regions of physical interest on the complex k–plane when the potentials are given in a tabular form. The latter are encountered in inverse scattering and supersymmetric transformations. To investigate the effects of resonances on the analytical properties of the potential, we employed the Marchenko inverse scattering method to construct, phase and bound state equivalent local potentials but with different resonance spectra. It is shown that the inclusion of resonances changes the shape, strength, and range of the potential which in turn would modify the bound and scattering wave functions in the interior region. This could have important consequences in calculations of transition amplitudes in nuclear reactions, which strongly depend on the behaviour of the wave functions at short distances. Finally, an exact method to obtain the Jost solutions and the Jost functions for a repulsive singular potential is presented. The effectiveness of the method is demonstrated using the Lennard–Jones (12,6) potential.

1 Introduction

Interaction potentials between colliding nuclei are widely used to describe scattering and spectral data. For practical reasons, they are expressed in terms of quite simple analytic and local forms of specific shape with parameters adjusted to fit the

[1] Permanent address: Department of Theoretical Physics, University of Thessaloniki, Thessaloniki GR-54006, Greece.

scattering cross section well which means that the relevant scattering wave functions are asymptotically correct. Such potentials, however, do not guarantee that their off–shell characteristics are sufficiently good to describe equally well reactions that depend on the behaviour of the wave function in the interior region. Examples of such reactions are the electro–disintegration and photo–disintegration processes which depend crucially on the bound and scattering wave functions at all distances.

An alternative way to construct local nucleus–nucleus potentials is via inverse scattering techniques. The inversion potential in this case is directly related to the available information of the scattering phase shifts and of bound states. In the inverse scattering method at a specific partial wave ℓ (fixed–ℓ inversion) [1–3] and in the absence of bound states, the constructed potential is unique. When bound states are present one may construct an infinite number of potentials which are spectrum and phase equivalent at all energies. This is achieved by choosing arbitrarily the bound states normalization constants which are not available from experiments. However, the asymptotic normalization constants determine the shape and range of the potential which in turns affects the distribution of resonances in the k–plane and vice versa. This emphasizes the importance of taking resonances into account in constructing effective interactions which are usually ignored.

One of the main reasons for omitting the resonances is the lack of experimental information on their positions and widths especially for broad resonances. In the past, this was aggravated by the absence of an exact and yet simple method to study the analytical properties of the corresponding amplitude which could facilitate their incorporation into the potential construction. Recently, however, a method for direct calculation of the Jost function in the complex k–plane, has been developed [4–8] which is both exact and quite simple and thus it could be used, to incorporate in the potential construction the resonance poles as well.

The method is implemented via a complex rotation of the coordinates which requires knowledge of the potential off the real axis in the r–plane. This poses no problem when the potential is given in an analytic form. However, there are cases, such as the aforementioned inverse scattering method, in which the resulting potential is given numerically. In this paper, we show how the Jost function method of Refs. [4–8] can be extended to deal with such potentials.

The method, in the form developed in the aforementiond references, cannot be directly applied to potentials which are more singular than $1/r^2$ at the origin. Interatomic and inter-molecular are examples of this type of forces which are strongly repulsive at short distances due to the overlap of the electron clouds. It is, therefore, desirable to extend the Jost function method to potentials of this kind and thus investigate the analytical properties and the importance of resonances in atomic and molecular systems as well.

In Sect. II we describe our formalism by briefly recalling the Marchenko inversion and the Jost function method for locating resonances. In the same section the extension of the latter method to singular potential is described. In Sect. III we present our results while our conclusions are given in Sect. IV.

2 Formalism

2.1 Inverse Scattering Method

In the Marchenko inversion scheme [1–3] the potential $V_\ell(r)$, for each partial wave ℓ, is obtained from the relation

$$V_\ell(r) = -2\frac{\mathrm{d}K_\ell(r,r)}{\mathrm{d}r} \tag{1}$$

where the function $K_\ell(r,r')$ satisfies the Marchenko fundamental integral equation

$$K_\ell(r,r') + \mathcal{F}_\ell(r,r') + \int_r^\infty K_\ell(r,s)\mathcal{F}_\ell(s,r')\mathrm{d}s = 0\ . \tag{2}$$

The kernel $\mathcal{F}_\ell(r,r')$ of this equation is related to the S–matrix $S_\ell(k)$, and thus to experiment, via

$$\mathcal{F}_\ell(r,r') = \frac{1}{2\pi}\int_{-\infty}^{\infty} h_\ell^{(+)}(kr)\left[1 - S_\ell(k)\right]h_\ell^{(+)}(kr')\mathrm{d}k - \sum_{n=0}^{N_b-1} A_{n\ell}h_\ell^{(+)}(b_n r)h_\ell^{(+)}(b_n r'), \tag{3}$$

where $h_\ell^{(+)}(z)$ is the Riccati–Hankel function, N_b is the number of bound states, and $A_{n\ell}$ is the asymptotic normalization constant [3] for the nth bound state with energy $E_b^{(n)} = -\hbar^2 b_n^2/2\mu$ where ib_n lies on the positive imaginary axis of the k–plane. The $A_{n\ell}$ can be expressed in terms of the relevant Jost solution $\mathrm{f}_\ell^{(+)}(k,r)$

$$A_{n\ell}^{-1} = \int_0^\infty \left[\mathrm{f}_\ell^{(+)}(ib_n, r)\right]^2 \mathrm{d}r\ . \tag{4}$$

The S–matrix needed in Eq. (3) can be parametrized using the convenient rational ansatz,

$$S_\ell(k) = \prod_{i=1}^{\infty}\frac{k+a_i}{k-a_i}\ , \tag{5}$$

i.e. using an infinite number of simple poles and zeros. In practice the number of a_i in the above formula is limited to N which is sufficiently large to reproduce the input scattering phase shifts and bound states. The rational parametrization reduces the Marchenko inverse scattering procedure to an algebraic problem since the kernel of Eq. (2) becomes separable; this can easily be seen if one performs the integration in Eq. (3) using the residue method.

In the absence of bound states the above scheme is unique, *i.e.*, once a good fit to the data from $(0,\infty)$ is achieved, one and only one potential can be obtained. In the presence of bound states, however, the potential is not unique as it depends on the choice of the asymptotic normalization constants $A_{n\ell}$ which are not provided

by experiment. When $A_{n\ell}$ are chosen according to Eq. (4) or, equivalently, obtained via the Jost function $f_\ell(k)$,

$$A_{n\ell} = \left[i \frac{f_\ell(-k)}{\mathrm{d}f_\ell(k)/\mathrm{d}k} \right]_{k=ib_n} , \tag{6}$$

the resulting potential is unique and has the shorter range [3]. Any other choice can lead to an equivalent local potential which reproduces the same on–shell data but it has different shape and range. ¿From Eq. (6) it is clear that the normalization constants can be determined from the knowledge of the Jost function. In the case of rational parametrization Eq. (6), the $A_{n\ell}$ can be easily obtained as the Jost function also assumes the parametrization

$$f_\ell(k) = \prod_{i=1}^{\infty} \frac{k - \alpha_i}{k - \beta_i} . \tag{7}$$

where the parameters α_i and β_i can be extracted as described in [9].
The Jost function thus constructed approximates well the exact Jost function on a segment of the real axis of the k–plane. From this one should expect that it would be a good approximation off the real axis as well. Indeed, if two analytical functions coincide on any arc of a continuous curve, they coincide everywhere in the region of their analyticity [10].
There are at least two problems concerning such a parametrization. Firstly, the function (7) actually does not coincide with the exact Jost function on the real axis but can only be a good numerical approximation at certain points. How fast the deviations are growing when one moves away from the real axis is not known. Secondly, since instead of an infinite number of terms in Eq. (7), we have to truncate the product to a finite number of terms, not all α_i correspond to zeros of the exact Jost function. In other words, the fitting procedure employed to evaluate these parameters, may generates a number of unphysical zeros and poles which could be simply an artifact of the truncation.

2.2 Exact Method for Locating Resonances

The method we employ here for locating potential resonances belongs to the class of so-called complex energy methods which are based on a rigorous definition of resonances, namely, as zeros of the Jost function. Unlike most of the other methods of this class, which involve an expansion of the resonant wave function in terms of square–integrable functions, our method is based on a direct calculation of the Jost function at complex k by integrating exact differential equations equivalent to the Schrödinger equation,

$$\partial_r F_\ell^{(\pm)}(k,r) = \pm \frac{h_\ell^{(\mp)}(kr)}{2ik} V_\ell(r) \left[h_\ell^{(+)}(kr) F_\ell^{(+)}(k,r) + h_\ell^{(-)}(kr) F_\ell^{(-)}(k,r) \right], \tag{8}$$

the boundary conditions being

$$F_\ell^{(\pm)}(k,0) = 1 . \tag{9}$$

The new unknown functions $F_\ell^{(\pm)}(k,r)$ are subjected to the additional condition

$$h_\ell^{(+)}(kr)\partial_r F_\ell^{(+)}(k,r) + h_\ell^{(-)}(kr)\partial_r F_\ell^{(-)}(k,r) = 0 \ . \tag{10}$$

The sum of the products of the auxiliary functions $F_\ell^{(\pm)}(k,r)$ with the Riccati–Hankel functions,

$$\phi_\ell(k,r) = \frac{1}{2}\left[h_\ell^{(+)}(kr)F_\ell^{(+)}(k,r) + h_\ell^{(-)}(kr)F_\ell^{(-)}(k,r)\right] \ , \tag{11}$$

obeys the Schrödinger equation. The function $\phi_\ell(k,r)$ is the so-called *regular solution* which vanishes near $r = 0$ exactly like the Riccati–Bessel function, *i.e.*

$$\lim_{r\to 0} \phi_\ell(k,r)/j_\ell(kr) = 1 \ . \tag{12}$$

The Jost function, $f_\ell(k)$, can be obtained by comparing the asymptotic behaviour of the regular solution,

$$\phi_\ell(k,r) = \underset{r\to\infty}{\longrightarrow} \frac{1}{2}\left[h_\ell^{(+)}(kr)f_\ell^*(k^*) + h_\ell^{(-)}(kr)f_\ell(k)\right] \ , \tag{13}$$

with Eq. (11) expressed in terms of the auxiliary functions $F_\ell^{(\pm)}(k,r)$,

$$f_\ell(k) = \lim_{|r|\to\infty} F_\ell^{(-)}(k,r) \ , \tag{14}$$

In Ref. [5] it has been shown that the limit (14) exists for all complex k for which

$$\mathrm{Im}\, kr \geq 0 \ . \tag{15}$$

If r is real, the condition (15) is only satisfied for bound and scattering states but not for resonances. Therefore, to calculate $f_\ell(k)$ in the fourth quadrant we make the complex rotation of the coordinate in Eq. (8),

$$r = x\exp(i\theta) \ , \qquad x \geq 0 \ , \qquad 0 \leq \theta < \frac{\pi}{2} \ , \tag{16}$$

with a sufficiently large θ.
The above scheme works extremely well in locating bound, scattering, and resonant states as well in finding Regge poles and trajectories when the potential $V_\ell(r)$ is central, short range and it is given in analytic form. A generalization to non–central, multi–channel, and Coulomb–tailed as well as to singular potentials can be found in Refs. [4–6,8].

2.3 Jost Function for Singular Potentials

In the case of regular potentials the boundary conditions for Eq. (8) are given by Eq. (9). Going over to singular potentials, Eq. (12) does not hold anymore. Due

to the extremely strong repulsion, the regular solution vanishes much faster than $j_\ell(kr)$ when $r \to 0$. In fact, it vanishes exponentially [3] and therefore the conditions (9) must be modified accordingly. In order to find the exact behavior of the regular solution near the origin we apply the familiar semi-classical WKB method. Though the strong repulsion makes things rather complicated, it has the advantage that the criterion of the applicability of the WKB approximation is satisfied when $r \to 0$. Indeed, the WKB method works well when the local wavelength λ varies slowly, *i.e.*

$$|\mathrm{d}\lambda/\mathrm{d}r| \ll 1 \ . \tag{17}$$

It can be shown [11] that this derivative is given by

$$|\mathrm{d}\lambda/\mathrm{d}r| = \frac{1}{2}\left|\frac{\mathrm{d}V(r)}{\mathrm{d}r}[k^2 - V(r)]^{-3/2}\right| \ . \tag{18}$$

Assuming that $V(r)$ approaches its singularity near $r = 0$ monotonically, we can find an $r_{\min}$ that for all $r < r_{\min}$ the momentum in (18) is negligible, *i.e.* we may write

$$|\mathrm{d}\lambda/\mathrm{d}r| \underset{r\to 0}{\longrightarrow} \frac{1}{2}\left|\frac{\mathrm{d}V(r)}{\mathrm{d}r}[V(r)]^{-3/2}\right| \ . \tag{19}$$

When $r \to 0$, the right hand side of Eq. (19) for usual singular potentials tends to zero. For example, if

$$V(r) \underset{r\to 0}{\longrightarrow} g/r^n \ ,$$

the condition (17) is always satisfied for $n > 2$,

$$|\mathrm{d}\lambda/\mathrm{d}r| \underset{r\to 0}{\longrightarrow} \frac{n r^{\frac{1}{2}n-1}}{2\sqrt{g}} \longrightarrow 0 \ , \qquad \text{if } n > 2 \ .$$

Therefore, assuming that the necessary condition (17) is fulfilled and choosing a small enough $r_{\min}$, we can express the regular solution on the interval $(0, r_{\min}]$ using the WKB approximation (see, for example, Ref.[12]), viz.

$$\phi_\ell(k,r) = \frac{1}{\sqrt{p(r)}} \exp\left[i\int_r^a p(\rho)\mathrm{d}\rho\right] \ , \qquad r \in (0, r_{\min}] \ , \tag{20}$$

where the classical momentum $p(r)$ is defined by

$$p(r) \equiv \sqrt{k^2 - V(r) - (\ell + \frac{1}{2})^2/r^2} \tag{21}$$

and the upper limit a in the integral is an arbitrary value $a > r_{\min}$. Usually a is taken to be the inner turning point [12], but it is obvious from Eq. (20) that an additional integration from a to the turning point can only change the overall normalization of the solution which is not our concern at the moment. Thus, Eq.

(20) together with the derivative

$$\partial_r \phi_\ell(k,r) = \left\{ \frac{\mathrm{d}V(r)}{\mathrm{d}r} - 2\left(\ell+\frac{1}{2}\right)^2 r^{-3} \over 4[p(r)]^{5/2} - i\sqrt{p(r)} \right\} \exp\left[i \int_r^a p(\rho)\mathrm{d}\rho \right], \qquad (22)$$

$$r \in (0, r_{\min}]$$

can be used as boundary conditions for the regular solution of the Schrödinger equation at any point in the interval $(0, r_{\min}]$. To obtain the corresponding boundary conditions for the functions $F_\ell^{(\pm)}(k,r)$, we need to express them in terms of $\phi_\ell(k,r)$ and $\partial_r\phi_\ell(k,r)$. For this we can use Eq. (11) together with relation

$$\partial_r \phi_\ell(k,r) = \frac{1}{2}\left[F_\ell^{(+)}(k,r)\partial_r h_\ell^{(+)}(kr) + F_\ell^{(-)}(k,r)\partial_r h_\ell^{(-)}(kr) \right], \qquad (23)$$

which follows from (10). From (11) and (23) we find that

$$F_\ell^{(\pm)}(k,r) = \pm\frac{i}{k}\left[\phi_\ell(k,r)\partial_r h_\ell^{(\mp)}(kr) - h_\ell^{(\mp)}(kr)\partial_r\phi_\ell(k,r) \right] \qquad (24)$$

which is valid for any $r \in [0,\infty)$. Therefore Eqs. (24) taken at some point $r < r_{\min}$ with $\phi_\ell(k,r)$ and $\partial_r\phi_\ell(k,r)$ given by (20) and (22), provide us the boundary conditions, required in Eqs. (8), for singular potentials. It can easily be checked (by using $j_\ell(kr)$ for the regular solution near $r = 0$) that Eq. (24) gives the correct boundary conditions for regular potentials as well.

Alternatively to impose the boundary conditions on the functions $F_\ell^{(\pm)}(k,r)$ near the origin, one can simply solve the Schrödinger equation from a small r up to some intermediate point b where, using (24), the $F_\ell^{(\pm)}(k,b)$ can be obtained and propagated further on by integrating equations (8).

The use of more complicated boundary conditions at $r = 0$ does not change the condition (15) for the existence of the limit (14). Indeed, in deriving this condition we used only the behavior of the potential and the Riccati–Hankel functions at large distances [4,6]. Therefore, the Jost function for a singular potential can also be calculated by evaluating the function $F_\ell^{(-)}(k,r)$ at a large r. When we are dealing with resonances, i.e. working in the fourth quadrant of the k–plane, we need to integrate Eqs. (8) along the turned ray (16).

As can be seen from the WKB boundary conditions (20), the use of a complex r near the origin, makes $\phi_\ell(k,r)$ oscillatory from the outset. Although this does not formally cause any problem, in numerical calculations such oscillations may reduce the accuracy. To avoid this we solve Eqs. (8) from a small $r_{\min}$ to some intermediate point b along the real axis and then perform the complex rotation,

$$r = b + x\exp(i\theta), \quad x \in [0,\infty), \quad 0 \le \theta < \frac{\pi}{2}, \qquad (25)$$

Therefore, on the interval $[r_{\min}, b]$ we can use Eqs. (8) as they are, while beyond the point $r = b$ these equations are transformed to

$$\partial_x F_\ell^{(\pm)}(k, b + xe^{i\theta}) = \pm \frac{e^{i\theta} h_\ell^{(\mp)}(kb + kxe^{i\theta})}{2ik} V(b + xe^{i\theta}) \phi(k, b + xe^{i\theta}) \quad (26)$$

Though the complex transformation (25) is different from (16), the proof of the existence of the limit (14) given in the Appendix A.2 of Ref. [6] remains applicable here. Indeed, that proof was based on the fact that for $\mathrm{Im}\, kr > 0$ the Riccati–Hankel function $h_\ell^{(+)}(kr)$ decays exponentially at large $|r|$, and thus the derivative $\partial_r F^{(-)}(k, r)$ vanishes there and the function $F^{(-)}(k, r)$ becomes a constant. Under the transformation (25) the asymptotic behavior of the Riccati–Hankel function,

$$h_\ell^{(+)}(kr) \underset{r\to\infty}{\longrightarrow} -i \exp\left[i(kr - \ell\pi/2)\right] , \quad (27)$$

has only an additional r–independent phase factor $\exp(ikb)$ which does not affect the proof.

¿From the above, it is clear that we can identify the Jost function $f_\ell(k)$ as the value of $F_\ell^{(-)}(k, b + xe^{i\theta})$ at a sufficiently large x beyond which this function is practically constant. In the bound and scattering state domain, where $\mathrm{Im}\, k \geq 0$, one can choose any rotation angle θ allowed by the potential, including $\theta = 0$. In the resonance domain, however, where $k = |k| \exp(-i\varphi)$, $\varphi > 0$, the rotation angle θ must be greater or equal to φ. If the condition $\theta \geq \varphi$ is fulfilled, the value of the limit (14) does not depend on the choice of θ. This provides us with a reliable way to check the stability and accuracy of the calculations by comparing the results for $f_\ell(k)$ obtained with two different values of θ.

From Eq. (27) it is clear that the angular momentum appears only in the phase factor of the asymptotic behavior of the Riccati–Hankel functions and hence of the regular solution. Therefore, the use of any complex ℓ cannot change the domain of the k–plane where the limit (14) exists. This means that the Jost function can be calculated, for any complex angular momentum, using the same equations. Moreover, when looking for the Regge poles in the ℓ–plane, the complex rotation is not necessary because these poles correspond to real energies. Locating Regge poles as zeros of the Jost function in the complex ℓ–plane is easier than by calculating them via the S–matrix using three integration paths (in the r–plane) as suggested in Ref. [13].

2.4 Results

In the present work we firstly address the question of how the analytical properties of potentials given in tabular form, generated by inversion or Supersymmetric (SUSY) transformations [14] can be studied. To make an analytic continuation of them into the first quadrant of the complex r–plane, needed for the complex rotation, we fitted the potentials on the real axis by simple analytical forms with adjustable parameters and then considered r in these forms as a complex variable. Such an

approach to analytic continuation is based on a theorem of the complex analysis which states that if a function is analytic in a region and vanishes along any arc of a continuous curve in this region, then it must vanish identically in this region [10]. The obvious corollary of this theorem is that if two functions coincide on a curve, they coincide everywhere in the region of analyticity. Therefore, the analytical form which coincides with the tabulated function on the real axis should reproduce this function off the real axis as well. The question then arises if small numerical deviations in the potential on the real axis generate perceptible deviations of the position of the resonances. We have investigated this situation first by assuming the following analytic potential

$$V(r) = 5\exp\left[-0.25(r-3.5)^2\right] - 8\exp(-0.2r^2) \tag{28}$$

where the strength parameters are given in MeV and r in fm. The reduced mass μ is such that $\hbar^2/2\mu = 1/2\,\mathrm{MeV\,fm^2}$. The resonances and Regge trajectories of this potential were investigated in Ref. [5]. We then fitted the N points $V(r_i)$, $i = 1, 2, \cdots, N$ using the ansatz

$$V_{\mathrm{fit}}(r) = \sum_{n=1}^{N_1} a_n \exp\left[-b_n(r-c_n)^2\right] + \sum_{n=1}^{N_2} d_n \exp(-e_n r^2) \tag{29}$$

where the parameters were obtained using the MERLIN minimization program [15]. The minimization was stoped when the least square error on 120 points and $N_1 = 5$ and $N_2 = 4$ was of the order of 10^{-4} – a typical accuracy in these cases. This means that the fit to the analytic potential was between the third and fourth decimal in the whole region. With such a fit, all resonances found in Ref. [5] were recovered within three to five decimal points. Obviously the accuracy can be improved as the fit to the potential improves. One further comment is necessary: The form factors used for the fit restrict the use of rotation to a certain region only.

These test calculations show that the Jost function method is applicable and retains its effectiveness even when the potential is given numerically on the real axis. We can therefore use it to study the importance of incorporating physical two–cluster resonances in constructing a potential. This can be easily investigated by constructing Equivalent Local Potentials (ELP's) for a specific partial wave via inversion as described above and studying the implications of the implanted resonances. For this we use the nucleon–α potential of Dubovichenko et all [16] for the $\ell = 0$ partial wave

$$V(r) = -V_0 \exp(-\alpha r^2) \tag{30}$$

where $V_0 = 55.774\,\mathrm{MeV}$ and $\alpha = 0.292\,\mathrm{fm^{-2}}$. This is a deep potential that sustains an unphysical Pauli Forbidden State (PFS)[17] at $-9.73058\,\mathrm{MeV}$. This means that the Levinson's theorem, $\delta_0(0) - \delta_0(\infty) = \pi$, is fulfilled for this system. At large distances the radial wave function decays exponentially, $u_0(r) \longrightarrow_{r\to\infty} A_s \exp(-b_0 r)$, and the asymptotic normalization constant was found to be $A_s = 6.1603\,\mathrm{fm^{-1/2}}$.

By varying the asymptotic normalization constant we obtained a set of potentials which were fully phase shift and bound state equivalent but have different number

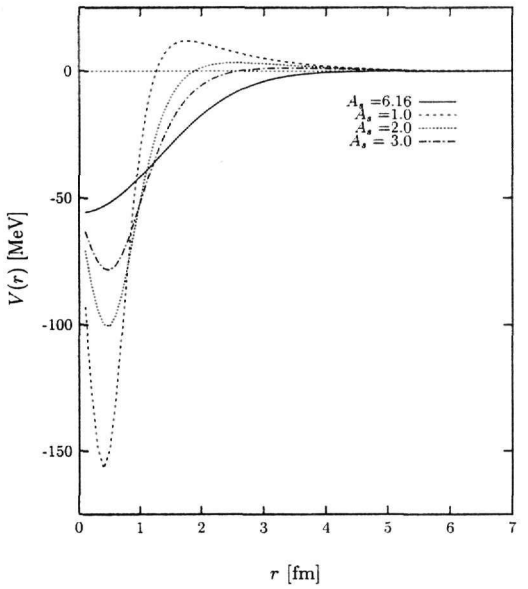

Fig. 1. Bound and phase equivalent potential for the nucleon – α interaction. These potential generate different resonance spectra.

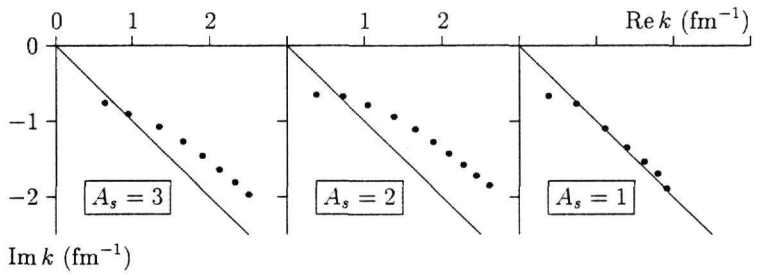

Fig. 2. Distribution of the Jost function zeros (filled circles) in the complex k–plane for the S–wave N–α potential for three different values of the asymptotic normalization constant A_s. The diagonal of the fourth quadrant represents the threshold boundary Re $E = 0$.

of potential resonances. These potentials are shown in Fig. 1. It is seen that for values of A_s less than the choice given by (4) ($A_s = 6.1603$), a hump appears in the interaction region which is higher as A_s becomes smaller while at the same time the well becomes deeper. For values larger than 6.1603 the potential is also of long range but without a hump. In the extreme case of $A_s = 0$ the potential becomes repulsive at all distances. This means that as $A_s \to 0$ resonances are generated and their appearance and position depend on the specific choice of A_s.

Using the ansatz (29) we fitted these potentials, with $N_1 = 5$ and $N_2 = 3$, the accuracy being again within a fourth decimal at all points meaning that correspnoding accuracy in reproducing the phase shifts was better than 0.0001 of a degree. We employed the analytical representations of these phase–equivalent potentials to locate the zeros of the Jost function in the fourth quadrant of the k–plane. The original potential (30), which is also a member of our set of ELP's, does not generate

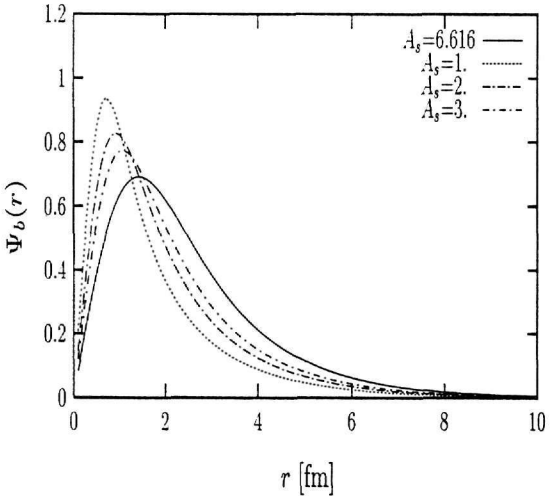

Fig. 3. Bound state wave functions generated by the potentials of Fig. 1

any physical resonances. All the zeros of the Jost function, which we found for this potential, are situated below the diagonal of the fourth quadrant of the k–plane and, therefore, represent sub–threshold resonances which are unphysical. The growth of the potential barrier when A_s decreases, indicates that some physical resonances should appear. In other words, when A_s becomes smaller some of the Jost function zeros should move up to the area above the threshold line. When, however, A_s is too small, the barrier transforms into a strong repulsive core, and the resonances should disappear. This can be seen in Fig. 2 where we present the distributions of the Jost function zeros for three phase–equivalent potentials corresponding to A_s equal to 3, 2 and 1.

At a first sight one can argue that the zeros of the Jost function practically have no effect on the scattering processes because they are far away from the real axis. These potentials, however, generate bound and scattering wave functions which have a different behaviour in the interior region. The bound state wave functions are shown in Fig. 3 while the scattering wave functions, for center of mass energy $E = 5\,\mathrm{MeV}$, are plotted in Fig. 4. The nodeless wave function for the SUSY potential is also shown. Since the interior region (within few fm) is of importance in describing various nuclear reactions, the existence and distribution of resonances cannot be ignored when the reaction observables are calculated. These differences are also a source of off shell differences in the corresponding scattering matrices which are manifested in three– and four–cluster calculations.

In order to evaluate the accuracy and efficiency of the method given in subsection 2.3 we apply it to the Lennard–Jones potential

$$V(r) = D\left[(d/r)^{12} - 2(d/r)^{6}\right] . \tag{31}$$

which is well–known in atomic and molecular physics. Combined with a rotational barrier, this potential supports narrow as well as broad resonant states (see, for example, Ref.[12]). To locate them, any method employed must be pushed to the extreme, thus exhibiting its advantages and drawbacks.

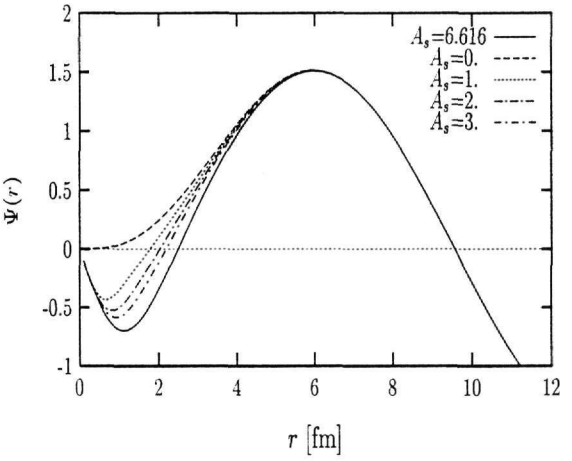

Fig. 4. Scattering wave functions generated by the potentials of Fig. 1 for $E = 5$ MeV. The $A_s = 0$ corresponds to the shallow SUSY potential that generates a nodeless wave function at short distances.

To compare our results with other calculations, we chose the same parameters as those of (31) used in Refs. [12,18], namely, $d = 3.56$ Åand with D varying from $5\,\mathrm{cm}^{-1}$ to $60\,\mathrm{cm}^{-1}$. The choice $D = 60\,\mathrm{cm}^{-1}$ together with the conversion factor $\hbar^2/2\mu = 8.7802375\,\mathrm{cm}^{-1}\text{Å}^2$ (which was used for all values of D) approximately represents the interaction between the Ar atom and the H_2 molecule [12]. In Table 1 the energies and widths of the first resonant states in the partial wave $\ell = 8$ are presented for different values of D. The results obtained with three other methods described in Refs. [12,18] are also given. The digits shown there are stable under changes of the rotation angle and thus they indicate the accuracy achieved. The third column of these tables, contains the results obtained in Ref. [12] using a Complex Rotation (CR) method which in some aspects is similar to ours. The authors of that reference perform the rotation directly in the Schrödinger equation and integrate it from $r = 0$ outwards and from a large $r_{\max}$ inwards. At the origin they use the WKB boundary conditions and at $r_{\max}$ they start from the Siegert spherical wave. In other words, the wave function is calculated using physical boundary conditions. In such an approach a resonance corresponds to a complex energy which matches the inward and outward integration. As indicated in Ref. [12], this method fails for broad resonances due to instability in the outward integration. In the fourth column the results obtained in Ref. [12] using the Quantum Time Delay (QTD) method are cited. This method is expected to be reliable for narrow resonances but its applicability to broad states is questionable. Finally, in the last column of Table 1 we give the results obtained in Ref. [18] using the Finite Range Scattering Wave (FRSW) method. The main idea of this method is based on the fact that while the scattering wave function cannot be expanded properly by a finite number of square integrable functions on an infinite range, it is possible to do so for a finite range.

The test calculations show that our method works well, especially for narrow resonances. Broad resonances can also be located. In contrast to the CR–method of Ref.[12], which was unstable for broad resonances corresponding to $D < 35\,\mathrm{cm}^{-1}$, we succeeded even in the case of $D = 5\,\mathrm{cm}^{-1}$ which generates an extremely broad

Table 1
Energies and widths of the lowest resonances, in the $\ell = 8$ partial wave, for the Lennard–Jones potential with different D. (D, $E_{\rm res}$ and $\Gamma_{\rm res}$ ($\rm cm^{-1}$)).

Ref.	This work		CR[12]		QTD[12]		FRSW[18]	
D	$E_{\rm res}$	$\Gamma_{\rm res}$	$E_{\rm res}$	$\Gamma_{\rm res}$	$E_{\rm res}$	$\Gamma_{\rm res}$	$E_{\rm res}$	$\Gamma_{\rm res}$
5	30	60						
10	27	42						
15	25.5	29.4						
20	24.5	24.8						
25	22.90	18.63						
30	21.193	13.70						
35	19.450	9.724	19.449	9.727	19.370	10.228		
40	17.6478	6.533	17.647	6.536	17.619	6.604	17.617	6.603
45	15.7768	4.039	15.777	4.039	15.769	3.992	15.769	3.990
50	13.81980	2.1833	13.820	2.183	13.819	2.143	13.818	2.142
55	11.744242	0.93915	11.744	0.939	11.744	0.926	11.743	0.926
60	9.4943275	0.264474	9.494	0.264	9.494	0.263	9.4934	0.263

state (its width is greater than the resonance energy by a factor of 2). Our results for small values of D, reproduce well the curve depicted in Fig. 3 of Ref. [12] which was produced semi-classically. The greater stability of the Jost function method as compared to the CR–method of Ref. [12] can be attributed to the use of the ansatz (11) for the regular solution. The Riccati–Hankel functions, explicitly extracted there, describe correctly all oscillations at large distances with the remaining functions $F_\ell^{(\pm)}$ being smooth. Another reason for this stability is the use of the deformed integration path given by Eq. (25) which enables us to avoid fast oscillations at short distances.

3 Conclusion

We demonstrated that for a potential given numerically the analytic properties of the corresponding Jost function in the complex k–plane can be obtained via fitting the potential by any analytic form that allows a complex rotation into the first quadrant of the complex r–plane. The scattering observables, the bound states, and the potential resonances can be calculated with a sufficient accuracy which is improved with an improved fit to the potential.

The phase shifts extracted from experimental data on the real k–axis, contain information about resonances in an indirect way. They "feel" the existence of resonances

only when they are close to the real axis (narrow resonances). The broad resonances, however, remain "unnoticed" and therefore a potential which is based on them, generates an S–matrix without the corresponding poles. However, even extremely broad resonances affect the behaviour of the wave function at short distances. This implies that an information on the distribution of resonances can be a clue for making a correct choice among very different potentials generating the on-shell S–matrix. Such information can, in principle, be obtained from various inelastic processes. For example, photo-excitation of a nucleus and its subsequent decay in two fragments A and B can reveal AB–resonances which are not "visible" in elastic AB–scattering. When a potential is constructed using theoretical phase–shifts, additional effort to locate broad resonances would exclude any ambiguities. For example, in the Resonating Group Model (RGM) [17] one has a complicated (nonlocal) potential and thus resorts to construction from nonlocal phase-shifts of an ELP with very simple simple form.

Finally, we presented an exact method for calculating the Jost function for singular potentials, for real or complex momenta of physical interest. We demonstrated, in the example considered, that the suggested method is sufficiently stable and effective even in the case of highly singular potentials.

References

[1] Z.S. Agranovich and V.A. Marchenko, *The Inverse Problem of Scattering Theory*, (Gordon & Breach, New York), 1964

[2] K. Chadan and P.C. Sabatier *Inverse Problems in Quantum Scattering Theory*, (Springer, New York), 1989.

[3] R.G. Newton, *Scattering Theory of Waves and Particle*, 2nd ed. (Springer, New York, 1982).

[4] S.A. Rakityansky, S.A. Sofianos, and K. Amos, Il Nuovo Cim. B **111**, 363 (1996).

[5] S.A. Sofianos and S.A. Rakityansky, J. Phys. A: Math. Gen. **30**, 3725 (1997).

[6] S.A. Rakityansky and S.A. Sofianos, J. Phys. A: Math. Gen, **31**, 5149 (1998).

[7] S.A. Sofianos, S.A. Rakityansky, and G.P. Vermaak, J. Phys. G: Nucl. Part. Phys. **23**, 1619 (1997).

[8] S.A. Sofianos, S.A. Rakityansky, and S.E. Massen, to appear in Phys. Rev. A (1999), available from the Los Alamos e-print archive as **nucl-th/9901023**.

[9] S.E. Massen, S.A. Sofianos, S.A. Rakityansky, and S. Oryu, Nucl. Phys. A. (in press), available from the Los Alamos e-print archive as **nucl-th/9906020**.

[10] P.M. Morse and H. Feshbach, *Methods of theoretical physics*, (McGrow-Hill Book Company, New York, 1953) p. 390.

[11] W.M. Frank and D.J. Land, Rev. Mod. Phys. **43**, 36 (1971).

[12] J.N.L. Connor and A.D. Smith, J. Chem. Phys., **78**, 6161 (1983).

[13] C.V. Sukumar and J.N. Bardsley, J. Phys. B **8**, 568 (1975).

[14] C.V. Sukumar, J. Phys. A **18**, L57 (1985); J. Phys. A **18**, 2937 (1985).

[15] D.G. Papageorgiou, I.N. Demetropoulos, and I. E. Lagaris, Comp. Phys. Comm., **109**, 227 (1998).

[16] S.B. Dubovichenko and A.V. Dzhazairov-Kakhramanov, Sov. J. Nucl. Phys. **51**971 (1990).

[17] K. Wildermuth and Y.C. Tang, *A unified theory of the Nucleus* (Brounsceving, Viliveg, 1977).

[18] H.W. Jang and J.C. Light, J. Chem. Phys. **99**, 1057 (1993).